Recent Insights into the Physics of the Sun and Heliosphere: Highlights from SOHO and Other Space Missions
IAU Symposium, Vol. 203, 2001
P. Brekke, B. Fleck, and J. B. Gurman eds.

Reconstruction of the Coronal Magnetic Field for Active Region NOAA 8151

S. Régnier

Institut d'Astrophysique Spatiale, Unité Mixte CNRS-Université Paris XI, Bâtiment 121, F-91405 Orsay Cedex, France

T. Amari

CNRS, Centre de Physique Thorique de l'Ecole Polytechnique, F-91128 Palaiseau Cedex, France

Abstract. The active region NOAA 8151 observed between February 11–13, 1998 exhibits a filament eruption linked to the disappearance of a sigmoidal structure. Using vector magnetograms from IVM (Mees Observatory, Hawaii), we perform a non linear force–free reconstruction of the coronal magnetic field above this active region. This reconstruction allows to determine the distribution of electric currents, the magnetic energy and the relative magnetic helicity. The reconstructed magnetic field lines are compared to the soft X–rays (SXT, Yohkoh) observations.

1. Introduction

The active region NOAA 8151 (AR8151) was observed on February 1998. A filament was observed in the Hα line, and a sigmoid appears in SXT/Yohkoh images (see Régnier et al., 1999). The disappearance of the sigmoid and of a part of the filament preceed a coronal mass ejection (CME). In Sect. 2, the vector magnetograms that we used to reconstruct the coronal magnetic field are detailed. The non linear force–free model detailed in Sect. 3 is compared to soft X-rays image (Sect. 4). Conclusions are drawn in Sect. 5.

2. IVM Vector Magnetograms

For this investigation, we use IVM (Imaging Vector Magnetograph ; Mickey et al., 1996) data providing the three components of the magnetic field (longitudinal, transverse, and azimuthal components). The field of view was $280'' \times 280''$. After the resolution of the 180°–ambiguity on the azimuthal component (Canfield, 1993), we select the part of the whole active region in which the total magnetic flux is close to zero (see Fig. 1 left). We also derive the vertical current on the photosphere $J_{z,obs}(x, y) = (\vec{\nabla} \times \vec{B}_{obs})_z$. We deduce the distribution of α_{phot} on the photosphere: $\alpha_{phot}(x, y) = J_{z,obs}(x, y)/B_{z,obs}(x, y)$ (see Fig. 1 right). The mean value of α_{phot} for the whole active region is 0.12 Mm^{-1}, for the negative polarity $2.18\,10^{-3}$ Mm^{-1}, and for the positive polarity 0.18 Mm^{-1}. Note that the small mean value of α_{phot} in the negative spot hides the strong positive and negative values of α_{phot} which may account for the return currents

https://doi.org/10.1017/S0074180900219761 Published online by Cambridge University Press

(expected in most physical process). The positive value of α_{phot} and the South location of the active region are in agreement with the statistical study made by Pevtsov et al. (1995).

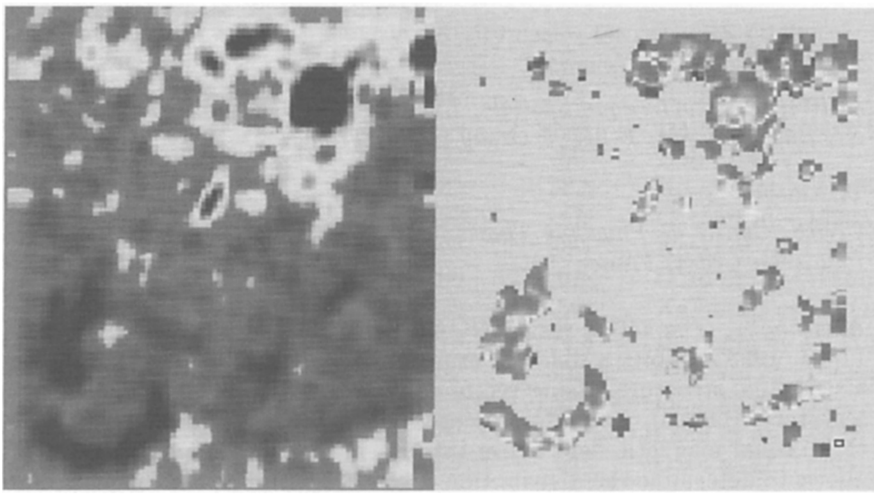

Figure 1. Vertical component of the magnetic field (left), distribution of α_{phot} on the photosphere (right).

3. Reconstruction Method

To reconstruct the coronal magnetic field, three assumptions are usually used: the potential (or current free) model, the linear and non linear force–free model. Here we only detailed the non linear force–free model (see Amari et al., 1996–1999) which satisfies: $\vec{\nabla} \times \vec{B} = \alpha \vec{B}$, and in which α is constant along a magnetic field line ($\vec{B} \cdot \vec{\nabla} \alpha = 0$). In Table 1, the value of α and the boundary conditions for the non linear force–free field are summarized: $B_z(x, y, z = 0)$ is the vertical component of the magnetic field given by the observations (Fig. 1 left) and $\alpha(x, y, z = 0)$ corresponds to the α measured on the photosphere (Fig. 1 right). We also compute the magnetic energy W and the relative magnetic helicity ΔH (see Amari & Luciani, 2000) : $W = 1.05\, 10^{25}\ erg$, $\Delta H = 5.28\, 10^{34}\ G^2 \cdot cm^4$.

Model	α	Boundary Conditions
Non Linear Force–free	$\alpha(x, y, z)$	$B_z(x, y, z = 0) = B_{z,obs}(x, y)$ $\alpha(x, y, z = 0) = \alpha_{phot}(x, y)$

Table 1. The value of α and the boundary conditions for the non linear force–free field.

4. Comparison between the observations and the non linear force–free model

In Fig. 2, we compare a soft X-rays image (11-Feb-1998 15:36:55 UT) to the non linear force–free field obtained with an IVM vector magnetogram (11-Feb-1998 17:35 UT). The sigmoid appears both on the soft X-rays image (Fig. 2 left) and in the reconstructed magnetic field model (Fig. 2 right).

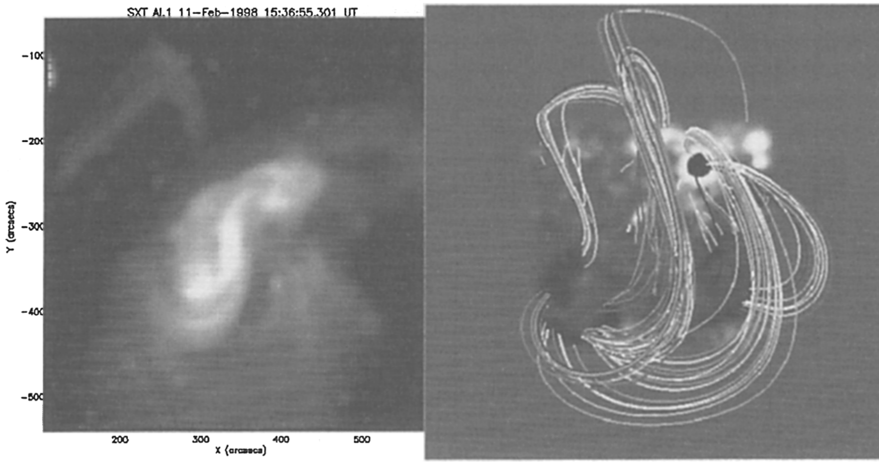

Figure 2. Comparison between SXT image in solar coordinates (left) and non linear force–free field in heliographic coordinates (right).

5. Conclusions

We reconstructed the coronal magnetic field of the active region NOAA 8151 using IVM vector magnetogram as boundary conditions, and compared to the soft X-rays image. One can see the good agreement between the sigmoidal structure seen in soft X-rays and the modeled field lines. The non–constant distribution of α on the photosphere justify that the best agreement between observations and models is obtained for the non linear force–free field. The magnetic energy ($\sim +40$ % of the magnetic energy for the potential case) is sufficient to trigger an eruptive event (Amari & Luciani, 1999a). The moderate absolute value of the magnetic energy ($\sim 10^{25}$ erg) may be consistent with the fact that the filament eruption was not linked to EIT flare.

Acknowledgments. Data used here from Mees Solar Observatory, University of Hawaii, are produced with the support of NASA grant NAG 5-4941 and NASA contract NAS8-40801.

References

Amari, T., Luciani, J.F., Aly, J.J., Tagger, M., 1996a, ApJ, 466, 39
Amari, T., Luciani, J.F., 1999a, ApJ, 515, 81
Amari, T., Luciani, J.F., Mikic, Z., Linker, J., 1999b, ApJ, 518, 57
Amari, T., Luciani, J.F., 2000, Phys.Rev.Lett, L6, 627
Canfield, R.C., 1993, ApJ, 411, 362
Mickey, D.L., et al., 1996, Solar Phys., 168, 229
Pevtsov, A.A., Canfield, R.C., Metcalf, T.R., 1995, ApJ, 440, 109
Régnier, S., Amari, T., Solomon, J., Vial, J.C., Mickey, D.L., 1999, Proc. 8th SOHO Workshop, ESA SP–446, p.571